Interactive Simulation of Realistic Fluid Movement Based on SPH Method

J L Miao[1], L J Long[1]*, Y H Miao[2], Y Qin[1]

1. Southwest Hydraulic Research Institute for Water Transport, Chongqing Jiaotong University, Chongqing 400016, China

2. National Engineering Research Center for Marine Aquaculture, Zhejiang Ocean University, Zhejiang 316022, China

ABSTRACT

With the continuous progress of computer simulation technology, fluid simulation has been developed rapidly, and it has been widely used in many fields, especially in engineering computation, game and special effects in movie. Nevertheless, with the increasing requirements of fidelity of the motion and interaction of subjects, fluid simulation requires more realistic simulation results. However, the motion of real fluid and objects is often difficult to be expressed by simple process, which can only be realized by the physical laws in the real world. Physical-based fluid simulation is one of the most challenging research issues due to its complexity in theory and computations. Among numerous fluid simulation models, Smoothed Particle Hydrodynamics (SPH) based fluid simulation is the most widely used meshless method to simulate the realistic fluid motion. As a simple and flexible method, SPH particle characteristics make it naturally suitable for fluid simulation modeling and feasible to deal with many fluid simulation computation problems in a robust and stable way. The SPH basic principle, kernel function, discretization scheme and boundary treatments are introduced. The fluid movement is solved by SPH method in accordance with Navier-Stokes equations. The accuracy and stability of the fluid solution equation was improved by correcting the pressure and velocity fields. Secondly, the water surface was modeled, and the rendering speed of the fluid surface was optimized by simplifying the fluid particles calculation. The SPH model is developed to simulate impulsive wave generated by dam-break and high-speed landslide. It shows the model can simulate the movement process of the fluid fragment and coalescence, and available to simulate the blood, volcanic explosion, and tsunami propagation.

1. INTRODUCTION

Fluid simulation has been the focus of computer graphics research in recent years. Due to the limitation of computational capacity, the early fluid simulation mainly used the method of parameter modeling. In 1986, Peachey expressed the wave function as a combination of a series of linear wave patterns and used particle system to simulate the waves. The reality of the results is poor. Tessendorf used the statistical FFT empirical model to describe the sea level with small amplitude in 1999. The above model is difficult for users to control, and it is difficult to simulate some complex and more detailed effects. In order to solve this problem,

*Corresponding Author: reduyuxn@163.com

many researchers turn to physics-based simulation methods, Kehl and de Haan use aerial terrain LiDAR point clouds of The Netherlands and complex computational fluid dynamics (CFD) models the interactive simulation and visualization of realistic flooding scenarios were performed [1]. Physical based fluid simulation can be roughly divided into two categories. One is the Euler method based on grid, such as based on FLUENT software, combined with RNG turbulence model and VOF method, two-dimensional landslide surge is simulated [2]. Yuan et al. [3] established a plane two-dimensional reservoir landslide surge FVM mathematical model under variable grid by using dynamic grid technology. The other is particle-based Lagrange method. Reeves first introduced particle system into the field of computer graphics in 1983 [4]. Particle system has been used to simulate spray splash and foam effect. In 1955, Stam et al. First introduced SPH smooth particle hydrodynamics method into computer graphics to simulate the diffusion of fire and other gases. Micky used SPH method to realize wave effect analysis in 2006 [5]. In recent years, SPH method has gradually become the main method of particle based Lagrangian method [6-8].

As one of the meshless methods, SPH (smooth particle hydrodynamics) regards the fluid as composed of many scattered particles with certain spacing, which is especially suitable for simulating transient large deformation problems such as smoke, fluid splash and surge [9-10]. In this paper, SPH method will be used to simulate dam break and surge flow process.

2. SPH METHOD

2.1. Navier-Stokes Controlling Equations

Fluid motion can be expressed by N-S equation [11-12]. The governing equation of Lagrangian is

continuity equation, $$\frac{D\rho}{Dt} = -\rho\nabla.\vec{v} \tag{1}$$

momentum equation, $$\frac{D\vec{v}}{Dt} = -\frac{1}{\rho}\nabla p + \vec{g} + \nu_0\nabla^2\vec{v} \tag{2}$$

where ρ = density of fluid particle, t = time, $\vec{v}$= velocity of particle, P = pressure, $\vec{g}$ = gravitational acceleration. ν_0 = coefficient of turbulent viscosity, $10^{-6}m^2/s$.

2.2. Discrete Format of SPH

In flow field simulation, the whole field becomes an expression of a series of particles and each particle can be expressed with ambient particles. And arbitrary macroscopic variable $f(x)$ can be calculated with interpolation by integral for a series of disorder particle value [13].

$$< f(x) >= \int_D f(x')W(x - x', h)dx' \tag{3}$$

where D = the whole domain, $f(x')$ = macroscopic variable value of the pre-set point, $W(x - x', h)$ = kernel function, which has two independent variables: the distance between particles $|x - x'|$ and smoothed length h. The function value at any point i can be regarded as a discrete form of SPH.

$$\langle f(x_i)\rangle = \sum_{j=1}^{N} m_j \frac{f(x_j)}{\rho_j} W(x - x_j, h) \tag{4}$$

where N = number of adjacent particles in the domain, m_j = mass of particle j, ρ_j = density of particle j.

According to equation (4), the SPH discrete format of the governing equation is:

$$\frac{d\rho_i}{dt} = \rho_i \sum_{j=1}^{N} v_{ij} \frac{m_j}{\rho_j} \frac{\partial W_{ij}}{\partial x_i} \tag{5}$$

$$\frac{dv_i}{dt} = -\sum_{j=1}^{N} m_j \left(\frac{p_i}{\rho_i^2} + \frac{p_j}{\rho_j^2} + \Pi_{ij}\right) \frac{\partial W_{ij}}{\partial x_i} + \vec{g} \tag{6}$$

Π is viscous term. In this paper, Morris et al (1997) proposed the formula,

$$\Pi_{ij} = \frac{4\nu_0 \vec{r}_{ij} v_{ij}}{(\rho_i + \rho_j)\vec{r}_{ij}^{\,2}} \tag{7}$$

where $v_{ij} = v_i - v_j$, is the speed difference between particles i and j, r_{ij} is the distance vector between the two particles.

By introducing artificial compressibility, the general incompressible fluid is regarded as compressible fluid. Monagham uses the method of artificially increasing the compressibility of fluid to construct the equation of state and directly give the relationship between density and pressure. It is simple to program for not solving Poisson equation of pressure [14].

$$p = B\left(\left[\frac{\rho}{\rho_o}\right]^{\gamma} - 1\right) \tag{8}$$

where ρ_0 = initial density of particle, γ = coefficient, $\gamma = 7$ for water. B is used to limit the maximum change of density, which is generally used as the initial pressure, $B = \frac{\rho_0 C^2}{\gamma}$. C is the artificial speed of sound, equals to 10 times maximum speed of total flow, $C = \sqrt{200gH}$, H is height of water surface.

The displacement of the particles:

$$\frac{d\vec{r}}{dt} = \vec{v} \tag{9}$$

Equations (5), (6), (8) and (9) constitute the discrete N-S equations based on SPH, and the complete iterative equations are formed by introducing the definite solution conditions.

2.3. Selection of Smooth Kernel Function

The smooth kernel function is a function of particle spacing $|x - x'|$and smooth length H. In addition to satisfying the Dirac δ function, the smoothed kernel function should also have some properties such as normalization, compactness and monotonous nonnegativity. Common kernel functions include Gaussian, splines of cubic, fourth and fifth. This paper chooses the simple quadratic kernel function to simulate impulsive wave,

$$W(r,h) = \alpha_D \left(\frac{3}{16}q^2 - \frac{3}{4}q + \frac{3}{4}\right) \qquad 0 \le q \le 2 \qquad (10)$$

where $q = (x - x')/h$, α_D = normalization constant, $\alpha_D = 2/(\pi h^2)$ for two dimensional problems.

2.4 Boundary Treatment Method

The wall boundary can be realized by Lennard-Jones repulsion method. The solid wall boundary is discretized into boundary virtual particles. The solid wall particles participate in the calculation of the governing equation. The wall adopts the sliding boundary, but their position is fixed in the simulation, that is, the displacement is set to 0. When the fluid particle is close to the solid wall, in order to prevent the fluid particle from crossing the solid wall boundary and cause computational collapse, the boundary particle exerts a central repulsion force of appropriate size on the fluid particle close to it, and the repulsion force only works at a close distance. The inlet boundary and outlet boundary are treated as special free boundary. The particle pressure at the interface is assigned as 0 or a certain external pressure value.

2.5. Numerical Solution

Particle search can adopt adjacent particle search method, tree search method, associated list search, etc. Firstly, calculate the density change of particles through the continuity equation, capture the free surface particles and correct the density of free surface particles, then calculate the pressure of particles through the equation of state, calculate the acceleration caused by external force, and then calculate the total acceleration of particles through the momentum equation. The particle density, velocity and position are updated by iterative method [15].

The time integration of discrete SPH equations generally adopts explicit schemes, such as fourth order Runge-Kutta method, leapfrog method, central difference scheme, Verlet difference scheme, etc. [16]. This paper adopts the prediction correction method. In order to ensure the convergence of the solution, the time step Δt CFL conditions shall be met.

3. FLOW SIMULATION ON DAM BREAK

In order to verify the effectiveness of SPH method in simulating dam break, which has large deformation flow of free surface fluid, the dam break process of water column in flume is simulated [17]. The test tank is a single width rectangular tank, with a length of 3.22m, a bottom slope of 0, a gate 1.2m away from the left, an initial upstream water level of 0.6m and a water density of 1000 kg/m^3. The water body is in static equilibrium at the initial time (Fig.1). Rapidly lift the gate to simulate water column dam break.

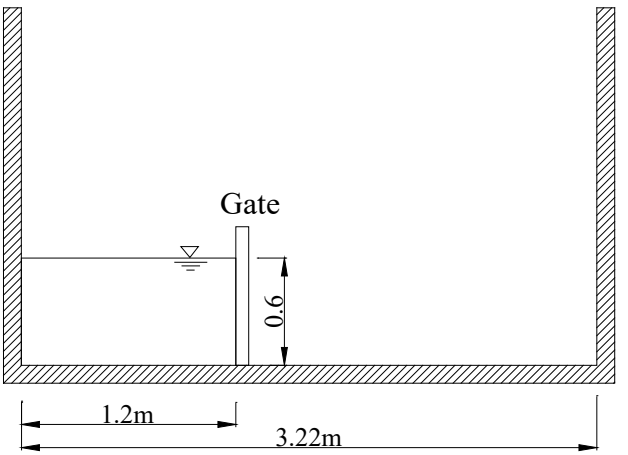

Fig.1. Experimental set-up and initial conditions

The whole calculation area is discretized, that is, the initial points are arranged as shown in Figure 2. The initial spacing of particles is d0 = 0.03m, and a total of 2065 particles are set, including 1580 liquid particles and 485 boundary particles. Smooth length H = 1.4 × d0. The time step Δt is given according to CFL conditions. The initial pressure of the particles is given by hydrostatic pressure.

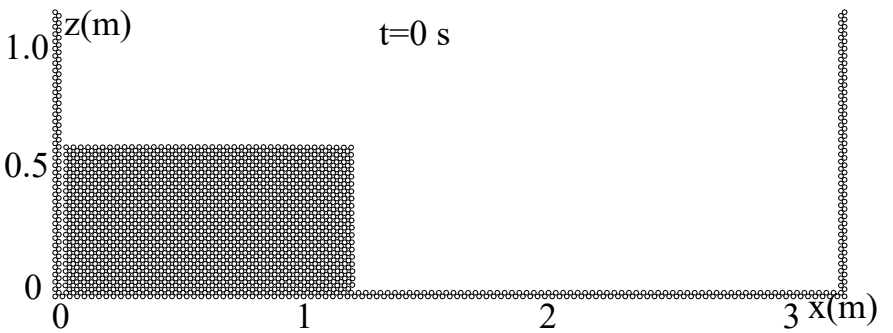

Fig. 2. Initial particle configuration

Figure 3 shows the movement of water particles in the whole tank after water column collapse. It can be seen from the figure that after the dam break, the water level drops rapidly, and the water body moves to the right at a high speed. When t = 0.5s, it reaches 2.7m downstream. When the front end reaches the right wall, it violently impacts the wall and climbs upward. When t = 1.0s, the water head formed by impact basically reaches the highest value. Then, under the action of gravity, the falling water body quickly falls and rolls over, and the falling water body strikes the water surface moving to the right at the bottom to form

closed bubbles (Fig. 3d). Due to the obstruction of the falling water body, the water particles moving to the right at the bottom of the trough will produce a second hydraulic jump before reaching the wall, and the height is greatly reduced compared with the previous one (Fig. 3e). After that, a number of bubbles of different sizes are generated in the right water body and gradually burst, forming a negative wave on the water surface and moving to the left.

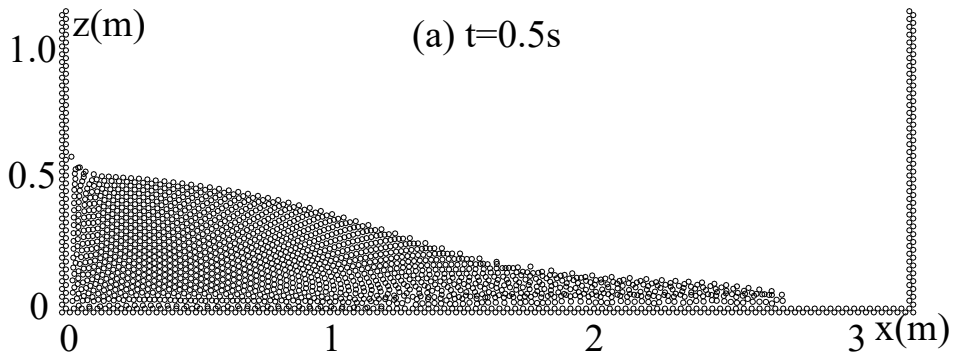

(a)

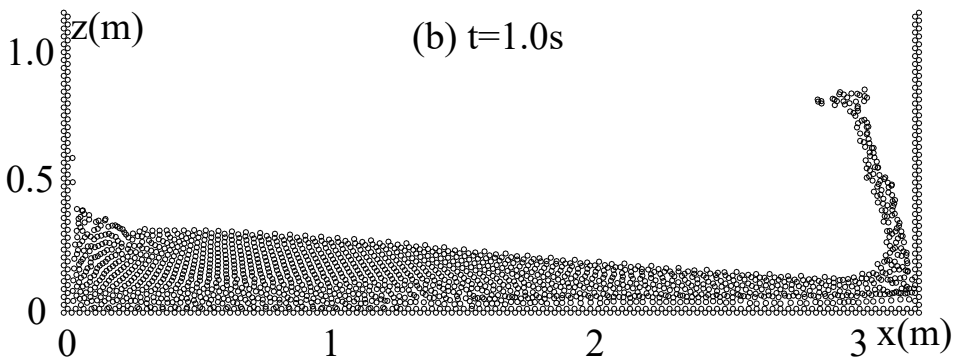

(b)

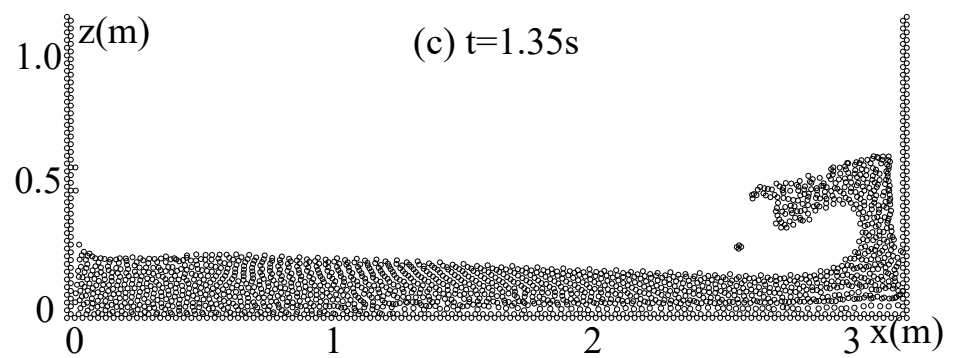

(c)

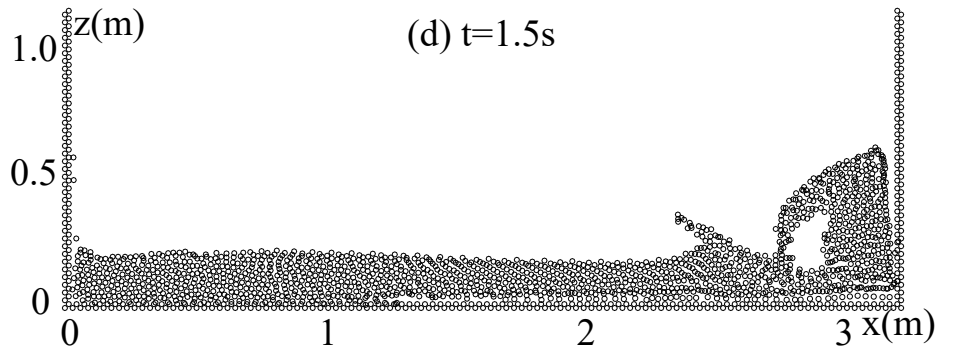

(d)

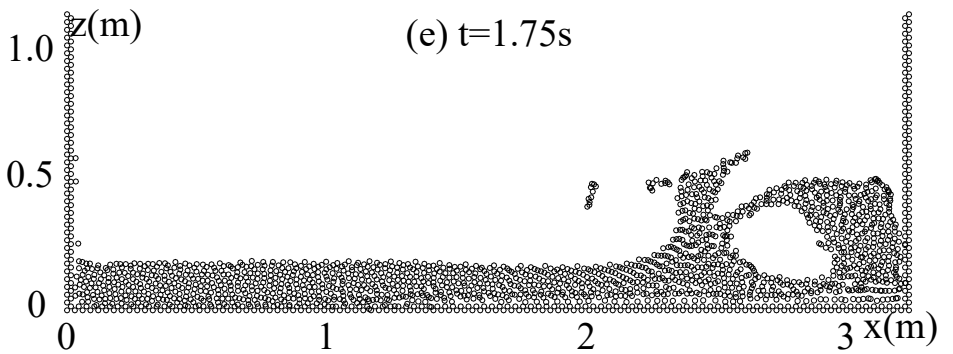

(e)

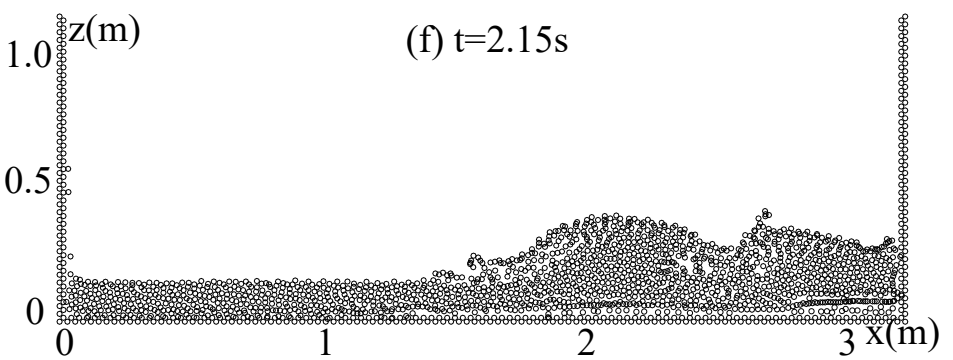

(f)

Fig. 3. Particle configurations after collapse at various time

4. SIMULATION OF IMPULSIVE WAVE GENERATED BY LANDSLIDE MOVEMENT

A landslide is shown in Figure 4. In SPH model, the water body is divided into many particles with mass attributes, and the bank slope is regarded as fixed particles. When the landslide moves underwater, the surface of the landslide is regarded as a movable boundary particle. In order to avoid the penetration of water particles, the solid wall particles on the bank slope are staggered into two rows, and the particle spacing is consistent with that of water particles. Particle spacing $\Delta x = \Delta z = 1m$. The total number of particles is 6806. The simulation time step $\Delta t = 0.001s$, which can be adjusted during operation.

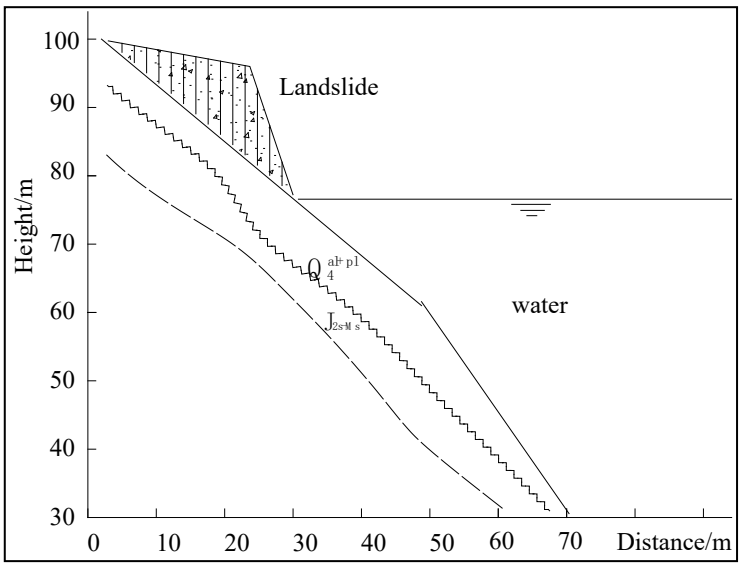

Fig. 4. Landslide geological profile

The landslide mass downward along the slide under the action of gravity, and its movement and deformation are simulated by establishing the soil motion equation [18]. When the front end enters the water body, it also needs to overcome the effects of fluid resistance and friction. The flow resistance value is $(1/2)m(dv/dt)$. The value of work done by the landslide to overcome the surface friction is $(1/2)c_d\rho_s v^2 S$. where M = mass of block, v = velocity of block, $c_d = 0.15 \sim 0.18$, ρ_s = liquid density, v = coefficient of viscosity, S = surface area on the water side [19].

4.1. Movement of landslide

The change of acceleration curve of landslide obtained by dynamic analysis is shown in Figure 5, the velocity change is shown in Figure 6. The simulation results show that the landslide slides with constant acceleration before entering the water, and the speed increases gradually. When t = 4s landslide starts underwater movement, the acceleration decreases slightly due to the increase of water resistance and the decrease of sliding force. As the bank slope becomes steeper, the sliding force increases, and the acceleration also increases. When $t = 11s$, the

acceleration reaches the maximum. After that, when the landslide mass moves at the bottom of the riverbed, due to the small slope, the sliding force decreases, and the acceleration decreases rapidly. At 12s, the acceleration is nearly 0. At this time, the speed reaches the maximum value, and the maximum sliding speed is 17.6 m/s. With the increase of fluid resistance, the velocity decreases rapidly when the acceleration is less than 0.

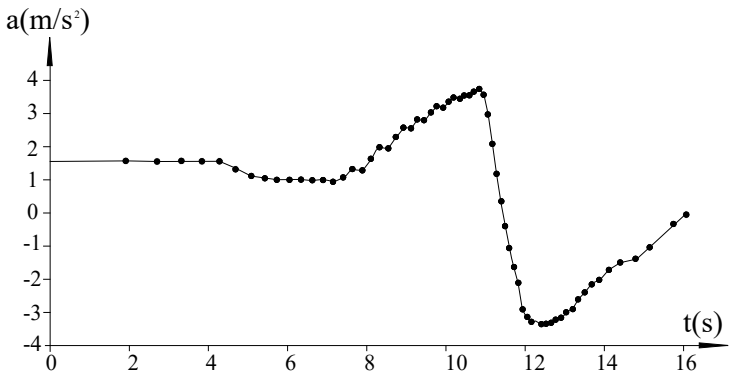

Fig. 5. Curves of sliding acceleration versus time

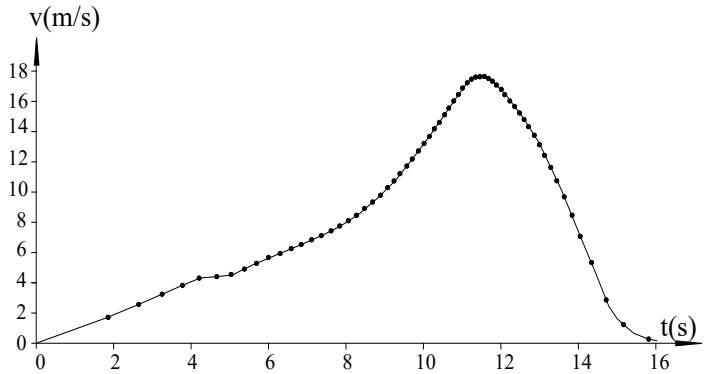

Fig. 6 Curves of sliding speed versus time

4.2. Impulsive waves

The change process of landslide surge is shown in Fig. 7 (a) - (e). When the landslide submerges underwater, it pushes the particles of adjacent water body to move rapidly to the right and raises the water level to form surge, and the positive wave on the water surface begins to form. When t = 10s, after the water wave reaches the right bank, the water flow continues to climb the coastal slope, and then the water flow falls down under the action of gravity and forms a negative wave to propagate to the left bank. After reaching the left bank, the wave is reflected to the right bank. After several reciprocating movements on both banks, the water surface oscillation gradually calmed down. When t = 12s, because the movement speed of the landslide is greater than the water flow speed, a large bubble is formed at the top of the landslide mass. With the gradual decrease of the movement speed of the landslide mass

along the river bottom, the bubble then collapses and causes obvious water air mixing. Figure 7 (c) shows in detail the water gas evolution process and the distribution of water particles through numerical simulation. From the change of water surface, the water surface surge height is 0 at the initial time, and then gradually increases. When t = 14.2s, the maximum wave height is 9.63m (Fig. 7 (d)), and then the maximum surge height gradually decreases smoothly. The maximum sliding distance obtained by simulation is 79.5 m.

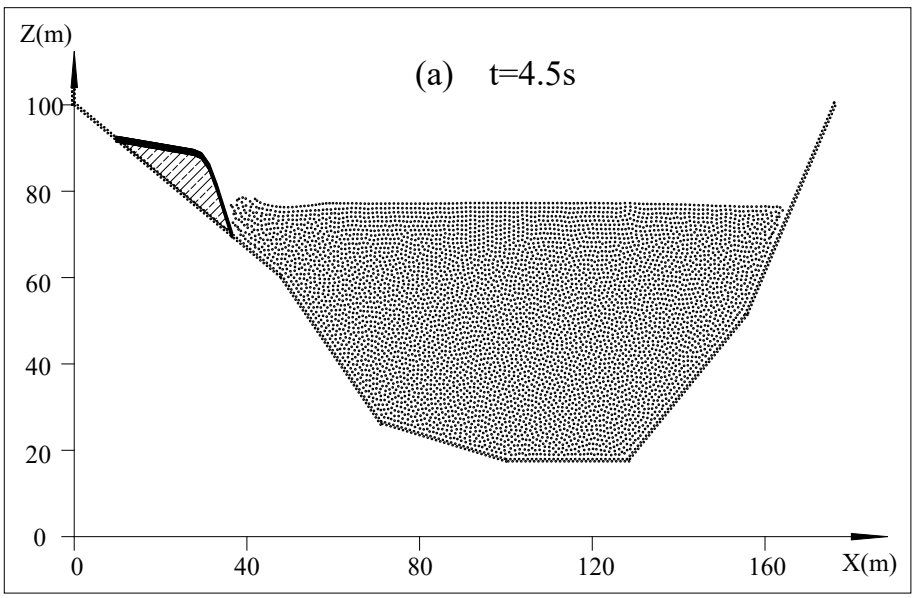

(a)

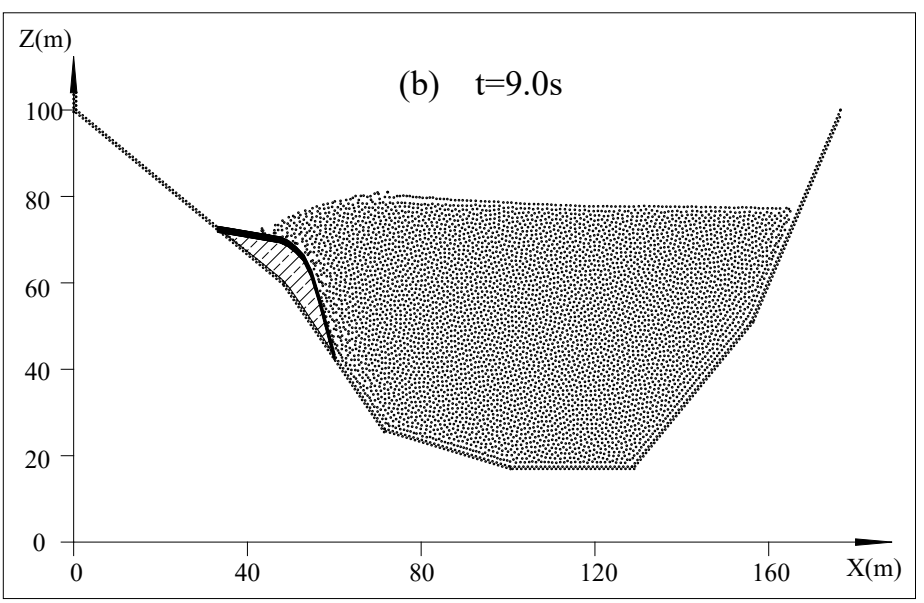

(b)

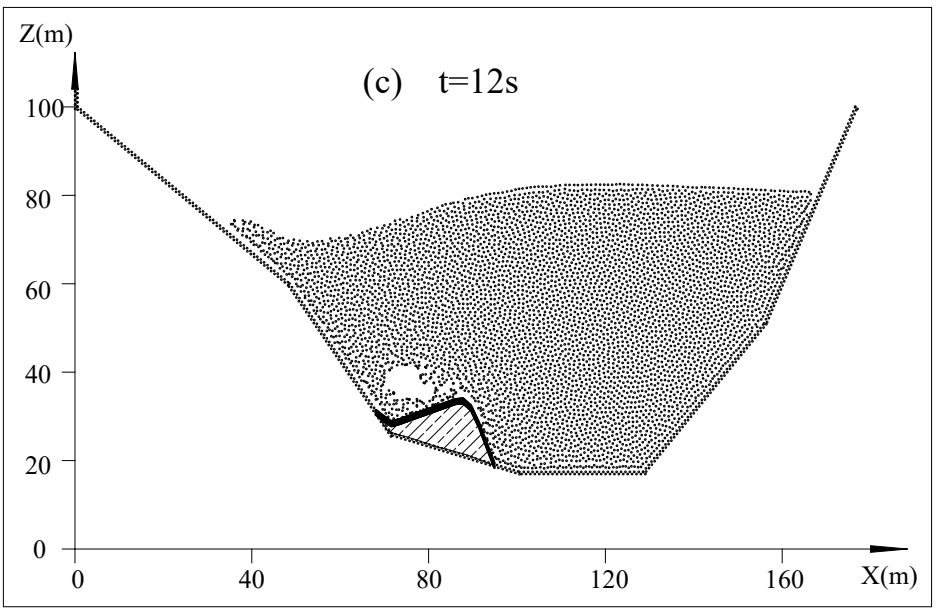
Z(m)
(c) t=12s
100
80
60
40
20
0
0
40
80
120
160
X(m)

(c)

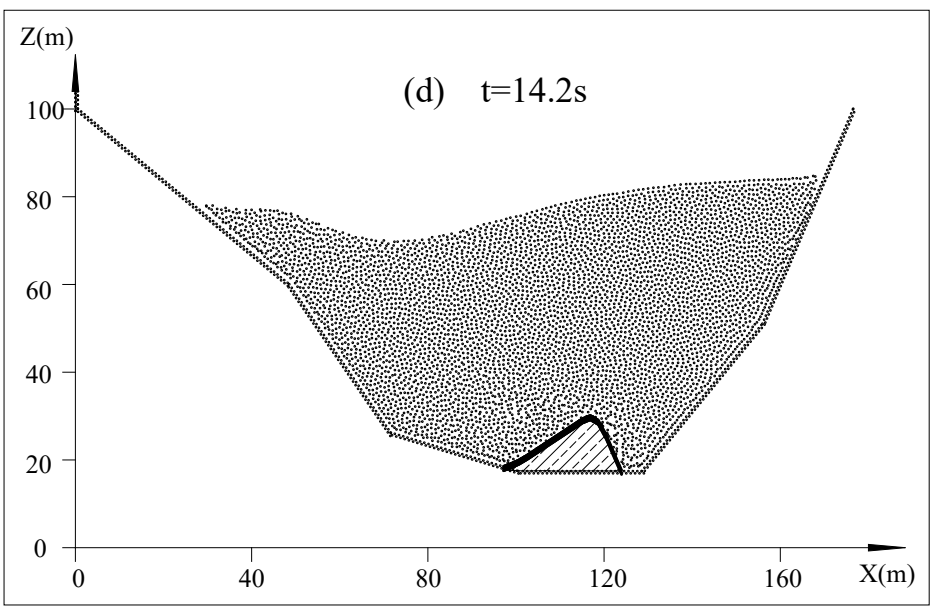
Z(m)
(d) t=14.2s
100
80
60
40
20
0
0
40
80
120
160
X(m)

(d)

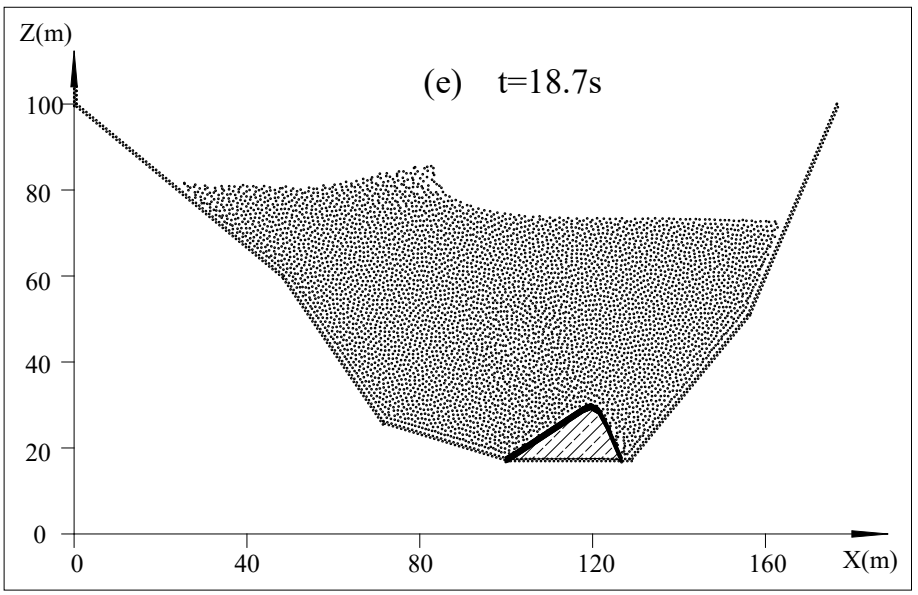

(e)

Fig. 7. Evolution of impulsive waves generated by landslide

5. CONCLUSIONS

The realistic simulation of natural scenes has always been a hot and difficult point in the research of computer graphics. Due to the sudden and ferocious characteristics of volcanic eruptions and debris flows, it is very difficult to shoot the scenes. Therefore, the realistic modeling and rendering of this sudden flow phenomenon is very necessary. Its research results can be applied to computer animation, computer games, film and television stunts, military simulation, virtual reality and popular science education. However, in the field of computer graphics, there are few realistic modeling and rendering of natural disaster scenes.

Based on the mechanical equations, this paper effectively simulates the complex free surface phenomena such as deformation, splash, fusion and bubble formation by dam break and high-speed landslide. It is feasible to trace the free surface and repeat the fluid fluctuation scene by rendering in the later stage. In order to enhance the realism of the scene, the next stage will carry out fine three-dimensional modeling of the flow scene objects and simulate the interaction between the fluid and the surrounding environment. At the same time, through the expansion of the solid-liquid two-phase flow model and post-processing such as rendering, the realistic simulation of disaster phenomena such as flood, landslide, avalanche, tornado, volcanic cloud and dust storm will be realized. SPH algorithm has great application prospects for creating realistic generation tools for natural scene simulation and developing special effect production software for fluid disaster scene.

REFERENCES

[1] Kehl, C., de Haan, G., "Interactive Simulation and Visualisation of Realistic Flooding Scenarios", In: Zlatanova, S., Peters, R., Dilo, A., Scholten, H. (eds) Intelligent Systems for Crisis Management. Lecture Notes in Geoinformation and Cartography. Springer, Berlin, Heidelberg, 2013, p. 79-93.

[2] Song, X.Y., Xing, A.G., Chen, L.Z., "Numerical simulation off two-dimensional water waves due to landslide based on FLUENT", Hydrogeology & Engineering Geology, 2009, 36(3): p.90-94.

[3] Yuan, J., Zhang, X.F., Zhang, W., "Horizontal 2-D flow model with variable grid for simulating surges due to landslide in reservoirs", Advances in Water Science, 2008, (4): p.546-551.

[4] Zhang, G.P., Zhang, M., Shao, X.Q., Wu, Z.H., "Realistic modeling and rendering of hydraulic erosion terrain," Journal of graphics, 2020, 41(2): p.169-177.

[5] Zhang, L.F., Zhang J.M., "A Comparative Study of SPH and LBM Methods for Numerical Simulation of Dam-break Flow", China rural water and hydropower, 2020, (10): p.236-241.

[6] Mashayekhi, O., Shah, C., Qu, H., Lim, A., & Levis, P., "Automatically Distributing Eulerian and Hybrid Fluid Simulations in the Cloud", ACM Transactions on Graphics, 2018, 37(2): p.1-14.

[7] Tartakovsky, A.M., Trask, N., Pan, K., Jones, B., Pan, W., & Williams, J.R., "Smoothed particle hydrodynamics and its applications for multiphase flow and reactive transport in porous media", Computational Geosciences, 2016, 20(4): p.807-834.

[8] Winchenbach, R., Hochstetter, H., Kolb, A., "Infinite continuous adaptivity for incompressible SPH", ACM Transactions on Graphics, 2017, 36(4): p.1-10.

[9] Hochstetter, H. and Kolb, A., "Evaporation and Condensation of SPH-based Fluids. Proceedings of the ACM SIGGRAPH/Eurographics Symposium on Computer Animation", Los Angeles, California, 2017, p. 1-9.

[10] Thuerey, N., "Interpolations of smoke and liquid simulations", ACM Transactions on Graphics, 2017, 36(1): p.1-16.

[11] Miao, J.L., Chen, J.Q., Zhang, Y.X., "Application of SPH method to studies on Free Surface Flows", Advance in science and technology of water resources, 2011, 31(3): p.20-23+39.

[12] Liu, G.R., Liu, M.B., Smoothed particle hydrodynamics-a meshfree particle method. Singapore: World Scientific Publishing Company, 2003, p: 26-32.

[13] Roubustsova, V., Kahavita, R., "The SPH technique applied to free surface flows", Computers & Fluids, 2006, 35(10): p.1359-1371.

[14] Gomez-Gesteira, M., Rogers, B.D., Dalrymple, R.A., & Crespo, A.J., "State-of-the-art of Classical SPH for Free-surface Flows", Journal of Hydraulic Research, 2010, 48(sup1): p. 6-27.

[15] Cheng, Z.Y., Xu, G.Q., Zhang, L.B., Xu, B., "Improved Algorithm for Realistic Fluid Interactive Simulation Based on Smoothed Particle Hydrodynamics", Journal of Wuhan institute of technology, 2019, 41(3): p.303-306.

[16] Yuan, Z.Y., Xu, B., Liao, X.Y., “Fast and precise surface tension for SPH-based fluid simulation”, Chinese journal of computers, 2019, 42(9): p.2062-2075.

[17] Pakozdi, C., Stansberg, C. T., Skjetne, P., & Yang, W., “Using a Simplified Smoothed Particle Hydrodynamics Model to Simulate Green Water on the Deck”, 31st International Conference on Ocean, Offshore and Arctic Engineering, Rio de Janeiro, Brazil, 2012, p.645-657.

[18] Ren, X.W., Tang, Y.Q., Dai, Y.X., Fang, Y., “Improved method for calculating landslide initial surge height”, Journal of Hydraulic Engineering, 2009, 40(9): p.1116-1119.

[19] Quecedo, M., Pastor, M., & Herreros, M. I., “Numerical Modelling of Impulse Wave Generated by Fast Landslides”, International Journal for Numerical Method in Engineering, 2004, 59(12): p.1633-1656.